

## ANALYSIS AND DISCRIMINATION OF SEDIMENTARY, METAMORPHIC, AND IGNEOUS ROCKS USING LASER-INDUCED BREAKDOWN SPECTROSCOPY

Ab. Kr. Rai,<sup>a</sup> G. S. Maurya,<sup>a</sup> R. Kumar,<sup>a</sup>  
A. K. Pathak,<sup>b</sup> J. K. Pati,<sup>a</sup> and Aw. K. Rai<sup>a\*</sup>

UDC 543.42;552.2

*This study deals with the analysis of rocks using laser-induced breakdown spectroscopy (LIBS) coupled with principal component analysis. The spectra of sedimentary, metamorphic, and igneous rock samples were recorded in the 200–900 nm spectral range. The atomic lines of elements such as Si, Ca, Mg, Fe, Na, and K along with lighter elements, namely C, H, N, and O, were observed in these spectra. Multivariate analysis in combination with LIBS was used to classify the samples. For principal component analysis, a  $12 \times 5849$  data matrix was formed using the results of LIBS. The plot of the analysis revealed similarities between the sedimentary and metamorphic rock samples compared with the igneous rock sample. Thus, the present study demonstrates that LIBS coupled with principal component analysis can become an important tool for rapid classification and in-situ discrimination of rock samples.*

**Keywords:** laser-induced breakdown spectroscopy, principal component analysis, sedimentary rock, metamorphic rock, igneous rock.

**Introduction.** The chemical characterization of minerals is useful for the classification of rocks and other planetary surfaces. Common analytical techniques used for the elemental analysis of rocks and minerals include atomic absorption and atomic emission spectrometry (AAS and AES), X-ray fluorescence (XRF) analysis, instrumental neutron activation analysis (INAA), laser ablation inductively coupled plasma mass spectrometry (LA-ICP-MS), proton induced X-ray emission (PIXE), etc. However, each of these techniques has inherent limitations [1–3]. Over the past two decades, laser-induced breakdown spectroscopy (LIBS) has emerged as a valuable tool for the elemental analysis of materials [4–6] due to its unique ability to monitor the major and minor constituents present in any phase (solid, liquid, or gas). In this technique, sample preparation (i.e., acid dissolution) is not required. Therefore, it is an eco-friendly approach offering advantages over other conventional analytical techniques [7]. Likewise, it is a multi-elemental analytical technique employing a high-energy source to create a high-temperature plasma on the sample surface. The constituents of the sample are vaporized, atomized, and excited into a hot plasma which emits atomic and ionic radiation characterizing the elemental composition of the sample [4–6]. The first use of LIBS for studying different geological samples involved mineral phases (vanadinite, pyrite, garnet and quartz) [8]. Jean et al. [9] demonstrated the feasibility of the identification of rocks on the surface of Mars based on LIBS spectra. Gondal et al. [10] developed a LIBS instrument for the analysis of volcanic rocks, and Giorgio [7] provided an exhaustive account of the applications of LIBS in the study of geological materials. The spectra emitted from the laser-induced plasma created on the surface of rocks are recorded without any sample preparation. They contain a plethora of information pertaining to the elemental concentration in the spectral range between 200 to 900 nm as a partly hidden complex data set. In addition, LIBS has an edge over the other conventional spectroscopic techniques as it analyzes lighter elements as well, such as O, C, H, etc. Multivariate statistical analysis was used [10, 11] to decipher information within the recorded data sets. The present paper deals with the complete elemental analysis of three representative rock types (sedimentary, metamorphic, and igneous) using *in situ* LIBS. LIBS and PCA were employed for the classification and discrimination of the chosen rock samples.

**Material and Method.** Igneous (granodiorite) and metamorphic (trondhjemite gneiss) rocks (Fig. 1a,b) were collected from the Bundelkhand craton, India. Sedimentary (arenite) rocks (Fig. 1c) were sampled from the Vindhyan Supergroup of

\*To whom correspondence should be addressed.

<sup>a</sup>University of Allahabad, Allahabad-211002, India; e-mail: awadheshkrai@rediffmail.com; <sup>b</sup>Ewing Christian College Allahabad, Allahabad-211003, India. Abstract of article is published in Zhurnal Prikladnoi Spektroskopii, Vol. 83, No. 6, p. 1010, November–December, 2016.

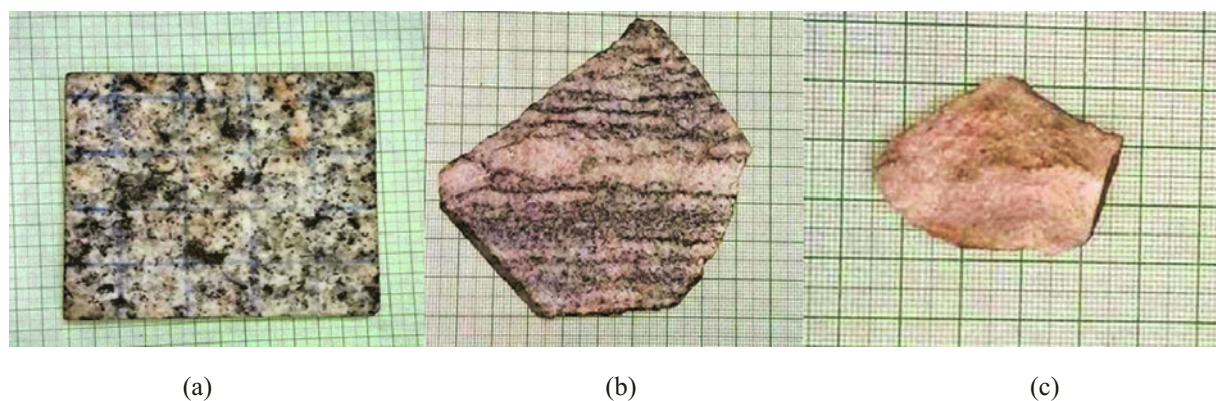


Fig. 1. Images of igneous (granodiorite) (a), metamorphic (trondhjemite gneiss) (b), and sedimentary (arenite) rocks (c).

rocks, India. Granodiorite is leucocratic, phenerocrystalline, coarse-grained, inequigranular, massive, rock, and composed of plagioclase (Ca-rich) feldspar, quartz, hornblende, apatite, zircon, and magnetite. Trondhjemite gneiss shows light (quartz + alkali feldspar) and dark (bitite + sphene + magnetite) bandings. Arenite is light gray, friable, and highly porous. All the samples were visibly fresh and devoid of major alterations.

The experimental setup to record the LIBS spectra of the rock samples was discussed in detail earlier [12, 13]. In the present study, LIBS spectra were collected from the plasma produced by focusing the 532 nm radiation of a Nd:YAG laser (Continuum Surelite III-10), on the rock samples, which delivers a maximum energy of 425 mJ and has a repetition rate of 10 Hz and a pulse width of 4 ns. The laser beam was focused on the sample surface using a plano-convex lens with a focal length of 15 cm which produced a plasma on its surface. The characteristic emission of the plasma was collected and transmitted to a spectrometer (Ocean Optics, LIBS 2000+ with 1.5  $\mu$ s fixed gate delay) equipped with a charge coupled device (CCD) using an optical fiber bundle. The obtained spectra were analyzed using OOI LIBS 2000+ software. The laser pulse energy and the pulse repetition rate were optimized to get a better signal to the background and the signal-to-noise ratio with optimized values of 20 mJ and 10 Hz, respectively.

**Results and Discussion.** *Elemental analysis.* The LIBS spectra of different samples were recorded from the plasma formed at the sample surface due to the high-power laser and sample interaction. The obtained spectral lines in the LIBS spectra of the samples were identified from the atomic spectroscopic NIST database [14]. The comparative typical LIBS spectra of rock samples recorded in the spectral range 200–500 nm are shown in Fig. 2. The spectral signatures of Al, Ba, Ca, Fe, Mg, Ti, Si, Sr, Na, K, C, H, O, and N are observed in the LIBS spectra of the analyzed rock samples. The wavelengths of the constituents (elements) observed in the LIBS spectra of the samples are summarized in Table 1.

The chosen rocks containing mainly silicate minerals are observed in the upper continental crust of the Earth and other planetary surfaces. The intensity of Si is prominent in the sedimentary rock sample compared with the igneous and metamorphic rocks. The microscopic study shows that mineral quartz ( $\text{SiO}_2$ ) comprises 95% (by volume) of the sedimentary rock (arenite), and this is supported by the LIBS results. In the igneous (granodiorite) rock, Ca has the highest intensity followed by the metamorphic and sedimentary rocks (Table 2). The petrographic study of granodiorite shows the presence of minerals rich in Ca (Ca-rich feldspar, hornblende, and apatite) which is demonstrated in the obtained LIBS spectra. Similar variations are observed for Ba, Sr, Al, and K (Table 2). The spectral line intensity of Mg, Fe, and Ti is higher in the igneous rock samples (Table 2). This strengthens the findings of LIBS in the present study. The spectral line intensity of Na is higher in the metamorphic samples. The spectral line intensity of O is the highest in the sedimentary samples, whereas C and H are the highest in the metamorphic ones (Table 2). Nitrogen is the highest in the sedimentary samples (Table 2). Thus, on the basis of the spectral intensities observed in the LIBS spectra, different types of rock samples can be characterized without involving destructive sample analysis and acid dissolution.

Tsuyuki et al. [15] showed that the intensity ratio of the ionic atomic line to the neutral one is proportional to the compressive strength of the target sample. Because of this, the speed of the shock wave generated in the hard target is larger than in the soft target, which boosts ionization. Therefore, in order to determine hardness, the intensity ratio of the ionic line of Fe (238.2 nm) to the corresponding neutral atomic line of Fe (344.0 nm) is calculated for different rock samples. This ratio is  $1.68 \pm 0.07$ ,  $0.75 \pm 0.12$ , and  $1.23 \pm 0.02$  for igneous, metamorphic, and sedimentary rocks, respectively. Thus,

TABLE 1. Spectral Wavelengths ( $\lambda$ , nm) Observed in Laser-Induced Breakdown Spectroscopic Spectra of Different Rock Samples

Element	Igneous rock	Metamorphic rock	Sedimentary rock
Al	226.9, 237.3, 308.2, 309.2	226.9, 236.7, 237.3, 308.2, 309.2, 394.3, 396.1	226.9, 236.7, 237.3, 257.5, 308.2, 309.2, 394.3, 396.1
Ba	230.4, 455.4, 493.3	230.4, 455.4, 493.3	230.4, 455.4, 493.3
Ca	422.6, 442.5, 443.9, 445.4, 315.9, 317.9, 370.6, 373.6, 393.2, 396.7	422.6, 443.4, 443.5, 445.4, 315.8, 315.9, 317.9, 373.6, 366.8, 393.2, 396.7	422.6, 443.4, 443.5, 445.4, 315.8, 315.9, 317.9, 373.6, 366.8, 393.2, 396.7
Fe	271.9, 344.0, 358.1, 373.7, 238.2, 239.5, 240.4, 249.3, 258.5, 259.8, 261.1, 273.9, 274.9, 275.5	271.8, 344.0, 358.0, 371.9, 373.7, 374.5, 375.8, 382.0, 404.5, 438.3, 234.3, 238.1, 239.5, 240.4, 249.3, 258.5, 259.8, 259.9, 260.7, 261.1, 273.9, 274.9, 275.5	271.8, 344.0, 358.0, 371.9, 373.7, 374.5, 374.9, 375.8, 382.0, 404.5, 438.3, 234.3, 238.1, 239.5, 240.4, 248.3, 249.3, 258.5, 259.8, 259.9, 260.7, 261.1, 273.9, 274.9, 275.5
Mg	285.2, 383.2, 383.8, 279.0, 279.5, 279.8, 280.2, 448.1	285.1, 383.2, 383.8, 279.4, 280.2, 448.1	285.1, 383.2, 383.8, 279.4, 280.2, 448.1, 383.2, 383.8, 279.4, 280.2, 448.1
Ti	363.5, 364.2, 365.3, 375.2, 430.5, 498.1, 499.1, 498.1, 499.1, 501.7, 501.4, 501.4, 506.4, 307.8, 308.8, 323.4, 323.6, 323.6, 323.9, 334.9, 336.1, 337.2, 338.3, 368.5, 375.9, 376.1	363.5, 364.2, 365.3, 375.2, 430.6, 499.1, 501.6, 501.3, 501.4, 506.4, 307.8, 308.8, 323.4, 323.6, 323.6, 323.9, 334.9, 336.1, 337.2, 338.3, 368.5, 375.9, 376.1	363.5, 364.2, 365.3, 375.2, 430.6, 499.1, 501.6, 501.3, 501.4, 506.4, 307.8, 308.8, 323.4, 323.6, 323.6, 323.9, 334.9, 336.1, 337.2, 338.3, 368.5, 375.9, 376.1
Si	220.7, 221.0, 221.6, 251.4, 252.8, 288.1	205.8, 220.7, 221.0, 221.6, 251.4, 251.6, 251.9, 252.3, 252.8, 288.1	205.8, 220.7, 221.0, 221.6, 250.6, 251.4, 251.6, 251.9, 252.3, 252.8, 288.1
Sr	460.7, 481.1, 216.6, 407.7, 421.5, 430.6	460.7, 481.1, 216.6, 407.7, 421.5, 430.6	460.7, 481.1, 216.6, 407.7, 421.5, 430.6
Na	589.5	589.5	589.5
K	769.8, 766.4	769.8, 766.4	769.8, 766.4
C	229.6	229.6	229.6
H	656.2	656.2	656.2
O	777.4, 844.6, 926.6	777.4, 844.6, 926.6	777.4, 844.6, 926.6
N	868.3	868.3	868.3

it is observed that igneous rocks have a higher ionic-to-neutral spectral intensity ratio compared with metamorphic and sedimentary rocks. Therefore, on the basis of LIBS, one can conclude that the igneous rocks studied here are the hardest among the three rock samples.

The amount of the ablated material also depends on the hardness of rock samples. This fact is also confirmed by measuring the diameter of the laser spot on the surface of different rock samples. The absolute diameter of the ablated area was measured using a Leica (DFC295) Zoom microscope. The measured diameter of the ablated spots (granodiorite, 156  $\mu\text{m}$ ; trondhjemite gneiss, 315  $\mu\text{m}$ ; arenite, 1590  $\mu\text{m}$ ) shows a distinct variation, and this corroborate our findings pertaining to the intensity ratio of the ionic-to-neutral atomic line observations discussed earlier.

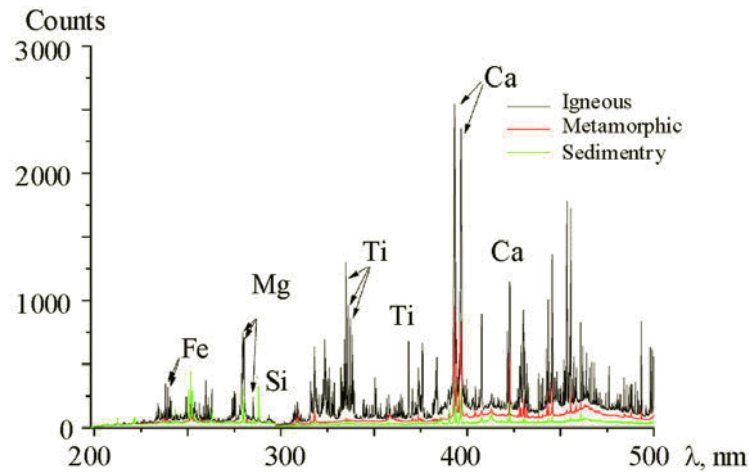


Fig. 2. Typical comparative laser induced breakdown spectroscopic spectra of igneous, metamorphic, and sedimentary rocks.

TABLE 2. Variation of Integrated Counts in Spectral Lines of Constituent Elements in Different Rock Samples

Line, nm	Igneous rock	Metamorphic rock	Sedimentary rock
Ca 422.6	3416 ± 121	1555 ± 198	619 ± 48
Ba 455.4	2002 ± 185	413 ± 76	34 ± 2
Sr 460.7	1001 ± 152	311 ± 29	82 ± 8
Al 308.2	150 ± 7	98 ± 6	64 ± 5
K 769.9	1339 ± 75	1063 ± 100	238 ± 30
Si 288.1	303 ± 6	276 ± 66	874 ± 141
Mg 285.2	563 ± 86	77 ± 6	100 ± 12
Ti 334.9	3855 ± 407	40 ± 5	352 ± 36
Na 589.0	4250 ± 384	5629 ± 813	1722 ± 182
O 777.1	1214 ± 91	985 ± 76	1319 ± 122
C 229.6	41 ± 6	47 ± 4	16 ± 5
H 656.2	1322 ± 203	1971 ± 138	1292 ± 220
Fe 248.3	53 ± 6	8 ± 1	15 ± 2
N 868.3	128 ± 15	106 ± 9	159 ± 17

*Principal component analysis.* On the basis of spectral line intensities, sample classification can be made only if the sample size is large. Multivariate analysis and principal component analysis (PCA) were used in the present study. PCA is a bilinear modeling method that provides a smaller number of latent variables, called principal components (PC). Each PC explains a certain amount of the total information contained in the original data, and the first PC contains the greatest source of information in the data set. Each subsequent PC contains less information than the previous one. By plotting PCs, important sample interrelationships can be revealed, which helps to interpret sample groupings, similarities, or differences.

A library of the LIBS spectra of different rock samples was used to form a data table in which each row represents an object (either individual or sample) and each column represents a descriptor (either measure or variable). Thus, a library

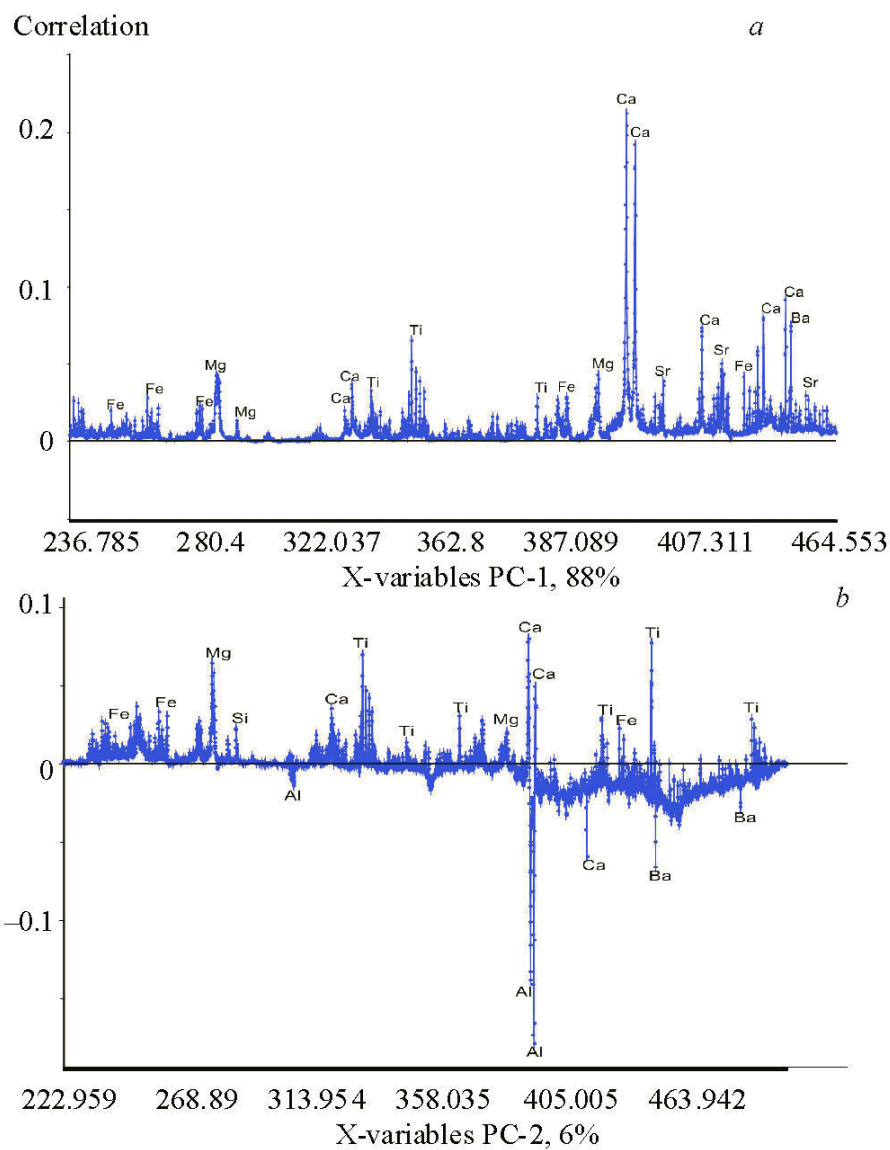


Fig. 3. Principal component analysis loadings plots of different rock samples.

of LIBS data along with Unscrambler PCA software (supplied by CAMO Software India Pvt. Ltd.) was used in the present study.

A  $12 \times 5849$  data matrix was formed using the obtained LIBS spectral features, and PCA was performed. The PCA plots are shown in Figs. 3a,b and Figs. 4a,b. Figures 3a,b show the loading plots of PCA. On the other hand, Figs. 4a,b demonstrate the score plots of PCA. The loading plots show the contribution of the spectral lines in the calculation of PC. Therefore, from Fig. 3a, it can be seen that Ca, Mg, Ti, Fe, and Sr participated in the calculation of PC1 as major components. Other elements shown in Fig. 3b participated in the calculation of PC2.

From Figs. 4a,b, it is clear that PC1 and PC2 explain the 94% variance among the data set. PC1 gives the maximum variance in the data set (88%), as shown in Fig. 4a, and PC2 gives the remaining variance of the data set (6%) (Fig. 4a). Figure 4a shows two-dimensional plots between PC1 and PC2, which clearly suggests that there are three types of rock samples from three different groups. It also reveals that the groups of sedimentary and metamorphic rock samples are relatively close. Figure 4b represents the three-dimensional plots of PC1, PC2 along with PC3, which shows three different groupings (present at three different planes) related to igneous, metamorphic, and sedimentary rock samples. It is another way of representation of the score plot in three dimensions. Figure 4c shows the explained variance. Thus, the present study demonstrates that LIBS coupled with PCA may be an important tool for the classification and *in situ* discrimination of rock samples.

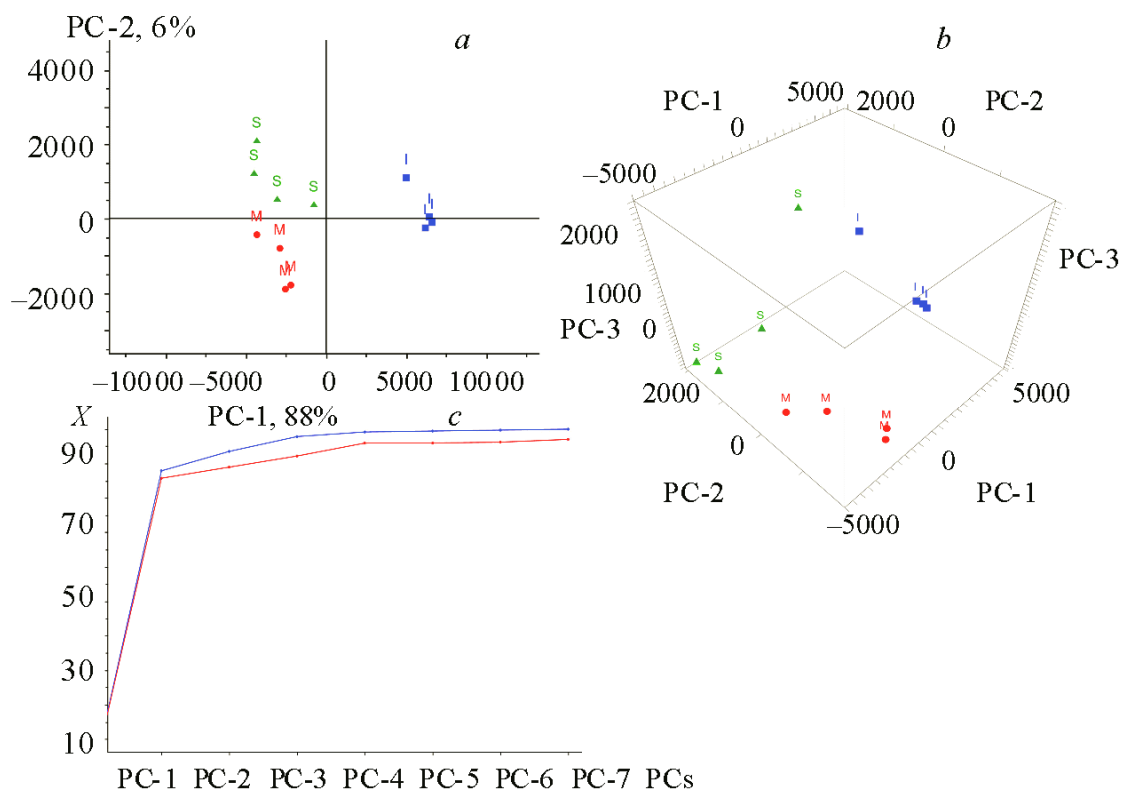


Fig. 4. Two-dimensional score plot of the first two principal components (a), three-dimensional score plot of the first three principal components (b), and explained variance plot (c).

**Conclusions.** The *in situ* investigation of different rock samples was made on the basis of the mineral profiling obtained using LIBS. The petrographic analysis of the samples, the variation in the diameter of the ablated spots, and the relative hardness variation findings clearly support the inferences from the LIBS study of geological materials. The LIBS data and multivariate analysis demonstrated similarities and differences between various rock types in terms of their elemental concentrations without involving lengthy sample preparation procedures. The present study demonstrated the potential of LIBS for the characterization and classification of rock samples.

**Acknowledgment.** The authors are thankful to UGC (CRET) for financial assistance at the University of Allahabad.

## REFERENCES

1. R. Tessadri, "Introduction to the Mineralogical Sciences. Pt 3: Analytical Techniques for Elemental Analysis of Minerals", *UNESCO Encyclopedia of Life Support Systems EOLSS* (2003); www.eolss.net
2. W. A. Deer, R. A. Howie, and J. Zussman, *An Introduction to the Rock-Forming Minerals*, 2nd ed., Wiley, New York (1992).
3. W. D. Nesse, *Introduction to Mineralogy*, Oxford University Press, New York (2000).
4. D. A. Cremers and L. J. Radziemski, *Handbook of Laser-Induced Breakdown Spectroscopy* Wiley, Chichester (2006).
5. J. P. Singh and S. N. Thakur, *Laser-Induced Breakdown Spectroscopy*, Elsevier Science (2007).
6. R. Noll, *Laser-Induced Breakdown Spectroscopy. Fundamentals and Applications*, Springer (2012).
7. G. S. Senesi, *Earth-Sci. Rev.*, **139**, 231–267 (2014).
8. J. J. Laserna, R. Fernández Reyes, R. González, L. Tobaría, and P. Lucena, *Opt. Express*, **17**, 10265–10276 (2009).
9. J.-B. Sirven, B. Salle, P. Mauchien, J.-L. Lacour, S. Maurice, and G. Manhe, *J. Anal. At. Spectrom.*, **22**, 1471–1480 (2007).
10. M. A. Gondal, M. M. Nasr, Z. Ahmed, and Z. H. Yamani, *J. Environ. Sci. Health, A*, **44**, 528–535 (2009).
11. S. M. Clegg, E. Sklute, M. D. Dyar, J. E. Barefield, and R. C. Wiens, *Spectrochim. Acta, B*, **64**, 79–88 (2009).

12. A. K. Rai, G. S. Maurya, R. Kumar, and A. K. Pathak, *Asian Mater. Sci. Lett.*, **3**, 123–126 (2014).
13. G. S. Maurya, A. Jyotsana, R. Kumar, A. Kumar, and A. K. Rai, *Phys. Scripta*, **89**, 075601 (2014).
14. National Institute of Standards and Technology, Electronic database; <http://physics.nist.gov/PhysRefData/ASD/lines form.html>
15. K. Tsuyuki, S. Miura, N. Idris, K. Hendrik, T. Jie, and K. Kagawa, *Appl. Spectrosc.*, **60**, No. 1, 61–64 (2006).